

INTERNATIONAL SOCIETY FOR SOIL MECHANICS AND GEOTECHNICAL ENGINEERING



This paper was downloaded from the Online Library of the International Society for Soil Mechanics and Geotechnical Engineering (ISSMGE). The library is available here:

<https://www.issmge.org/publications/online-library>

This is an open-access database that archives thousands of papers published under the Auspices of the ISSMGE and maintained by the Innovation and Development Committee of ISSMGE.

The paper was published in the proceedings of the 7th International Conference on Earthquake Geotechnical Engineering and was edited by Francesco Silvestri, Nicola Moraci and Susanna Antonielli. The conference was held in Rome, Italy, 17 - 20 June 2019.

Hybrid broadband seismic ground motions: Application to the city of Edessa in northern Greece

A. Kiratzi

Department of Geophysics, Aristotle University of Thessaloniki, Thessaloniki, Greece

Z. Roumelioti

Department of Civil Engineering, Aristotle University of Thessaloniki, Thessaloniki, Greece

K. Makra

OASP-ITSAK, Thessaloniki, Greece

N. Klimis

Department of Civil Engineering, Democritus University of Thrace, Xanthi, Greece

A. Koskosidi

ARUP, London, UK

ABSTRACT: Our motivation is to generate synthetic seismograms that could be incorporated in engineering seismology applications, in low-to-moderate seismicity regions. The case study is Edessa, located uphill and on top of a pile of post-alpine sediments. We use available records to validate our simulation parameters, and then adopt them for a scenario earthquake in the proximity of the city, i.e. rupture of a 12 km segment of the south-Almopia fault. Due to the near-fault conditions in our earthquake scenario set up, we use a hybrid approach. We perform site-specific response analysis for selected, typical for the city, soil profiles also accounting for soil properties variability. Our results indicate that Edessa is susceptible to considerable ground motion amplification, the intensity of which is variable within the city.

1 INTRODUCTION

The earthquake of 7 September 1999 Mw5.9, which occurred in the vicinity of Athens, the capital of Greece, revealed in the most severe way, that even moderate size events near urban regions can cause severe damage and life loss. Moreover, it is now clear to the geological community that the repeat rupture times of the known faults is not well constrained. In the mainland of Greece (Figure 1) the strain accumulation is taken up by a dense and segmented network of faults, many of which are blind, and not known unless an earthquake occurs. The available strong motion records, mainly sample the most seismically active regions, whereas there is a lack of records, for those regions that exhibit moderate to low-to-moderate seismicity, during instrumental times, although the historical memoirs clearly describe earthquake loss (Papazachos & Papazachou, 2003).

This leads to an insufficient knowledge regarding the intensity of ground motions especially for the urban regions, of these moderate seismicity zones. Motivated from the above discussion, we generate synthetic seismograms that could be incorporated in engineering seismology applications, in the absence of the appropriate recorded strong ground motions. The case study is Edessa, a city in northern Greece, which is significant to cultural heritage, densely populated, and located near active faults.

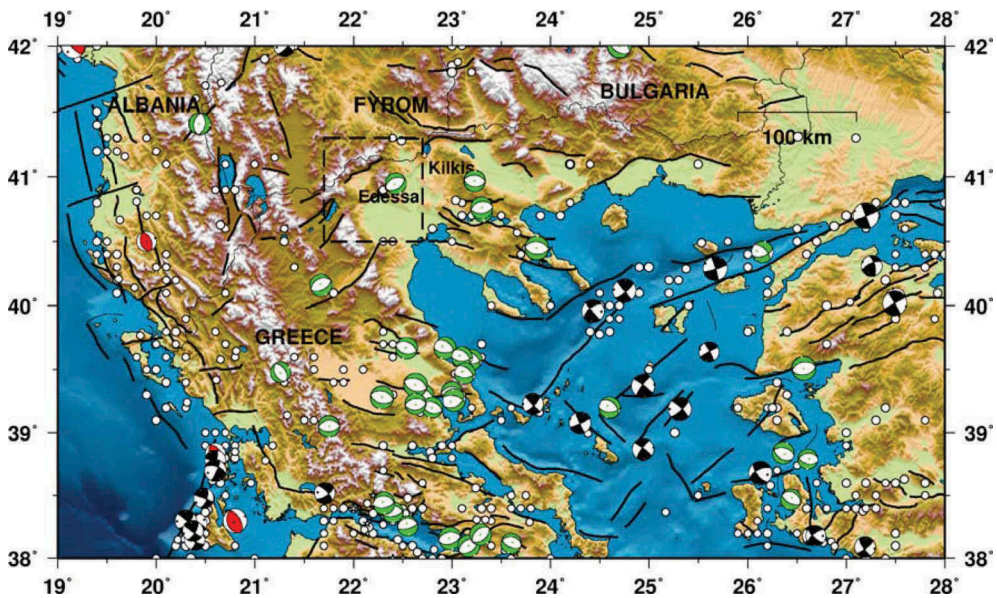


Figure 1. The region of northern Greece, depicting epicenters (circles) and focal mechanisms (beach balls) of earthquakes with $M \geq 5.8$, and distributed faults (black lines). The study area is shown within the dashed rectangle, depicting also the focal mechanism of the 21 Dec 1990 Mw6.1 earthquake.

2 TECTONIC SETTING

Edessa belongs to the zone of lowest design acceleration of the Hellenic Building Code (design acceleration 0.16g, with 10% probability of exceedance in 50 years). It is located uphill and on top of a pile of post-alpine sediments, which comprise travertine limestone overlain by fluvial, alluvial deposits. The city suffered moderate damage from the occurrence of the 21 December 1990 Mw 6.1 earthquake, located ~28 km NE. This event ruptured a blind normal fault, the Goumenisa Fault, previously unknown. It was recorded by an accelerograph located in Edessa (Prefecture building) with peak horizontal accelerations ~100 cm/s². The main active faults (Caputo et al., 2012; THALES-Project, 2015) that are in the proximity to the city of Edessa have as follows (Figure 2):

1. *North Almopia Fault Zone*: Its entire length is ~40 km and is segmented into three subfaults, which bounds the northern edge of the Almopia Basin.
2. *South Almopia Fault Zone*: This is a normal fault, dipping to the south, ~22 km in length, and the city of Edessa lies at a distance ~10 km from its western end. The inferred slip rate is ~0.2 to 0.4 mm/yr (Caputo et al., 2012). The dating of the filling material in the fault gauges indicates an age of ca. 8000 a. (Pavlidis, 1998)
3. *Goumenisa Fault*: The 21 December 1990 Mw6.1 earthquake is considered to have ruptured this 14 km long normal fault, which was not known before this earthquake, neither its signature was evident in the surface morphology (Panagiotopoulos et al., 1993). The earthquake caused 1 death and 60 injuries in the cities of Edessa and Kilkis, which both lie at ~30 km distance from the western and eastern end of the fault, respectively.

In the framework of previous work (Thales-Project, 2015) we have performed a detailed probabilistic seismic hazard analysis (PSHA) for the city of Edessa, taking into account all the seismogenic sources which contribute to the seismic hazard. The deaggregation results showed that the most significant hazard to the city is imposed by an earthquake of Mw6.05 located at a distance of 11 km. The predicted peak ground acceleration (PGA) values for a return period of 475 yrs, is of the order of 110 to 170 cm/s². This near-fault earthquake scenario is examined in the following sections.

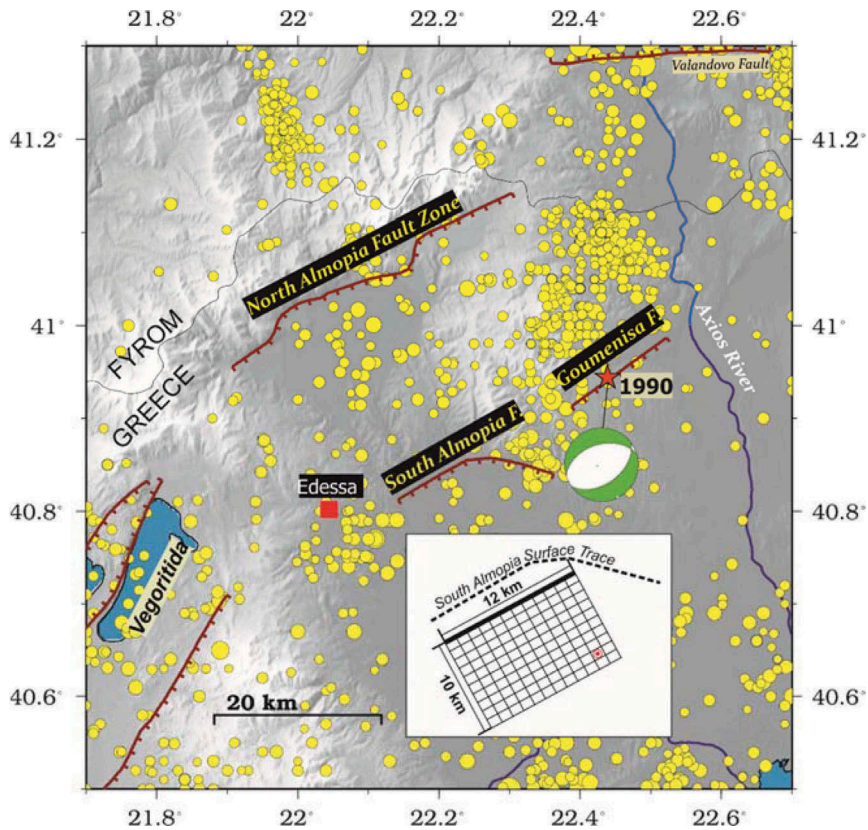


Figure 2. Location of the city of Edessa, within the study area, and main fault zones discussed in the text. The asterisk marks the location of the 21 December 1990 Mw6.1 earthquake, which was recorded by a 3-component accelerograph in Edessa and the beach ball its focal mechanism (strike 45°, dip 52°, rake -105°, GCMT). The inset shows the fault source model adopted in the scenario earthquake simulations, where the red circle marks the rupture initiation point.

3 SIMULATION OF GROUND MOTION FROM A SCENARIO EARTHQUAKE

3.1 Hybrid broad band ground motions for the South Almopia Fault scenario earthquake: Mw6.05 at R=11 km from the Edessa city

The scenario assumes rupture of a segment of the South Almopia Fault Zone (Caputo et al., 2012), which bounds the northern edge of the basin (Figure 2). We use a hybrid ground motion simulation approach: the low-frequency (LF) portion of synthetics is calculated using kinematic source modelling and deterministic wave propagation through a discrete wavenumber-finite element method, implemented in the COMPSYN code (Spudich & Xu, 2003); the high-frequency (HF) portion of synthetics is attained using a stochastic finite-fault simulation model and the EXSIM code (Motazedian & Atkinson, 2005; Boore, 2009). Subsequently, the hybrid broadband synthetics are obtained implementing a best pair match (Mai & Beroza, 2003), in the frequency domain, of the amplitude and phase spectra. In this manner, we compute rock-outcropping ground motions up to 4 Hz. Before proceeding to the scenario simulations, we validated our stochastic simulation parameters and the velocity model best describing the wave field, using the observed records of the 21 Dec 1990 Mw6.1 Goumenisa earthquake (Thales-Project, 2015). This earthquake (epicenter 40.95° N, 22.43° E) was recorded by an accelerograph located at the Building of Prefecture (EDE station) at the city of Edessa, at a distance of ~28 km from the eastern end of the fault.

We use a fault of 12 km × 10 km, in length and width, respectively, discretized into sub-faults of 1 km × 1 km. We place the rupture initiation point at the eastern end and deeper part of the fault, and we place the reference point (upper left edge of the fault) at coordinates 40.80° N, 22.16° E. The source geometry and the path parameters, adopted in the simulations, are as in Table 1. All the calculations, for both the stochastic and the deterministic parts of the ground motions are performed at the site of the Prefecture Building of Edessa. We computed first the stochastic part of the postulated ground motion using the EXSIM code (Figure 3a). The calculated PGA is ~180 cm/s², in accordance with the values obtained from the PSHA (THALES-Project, 2015).

Subsequently we calculated the LF frequency part (Figure 3b) of the ground motion (COMPSYN code) adopting the same source geometry, as before. We exhaustively tested the available for Greece velocity models, in order to compute the Green's functions. In fact, what we did, was to evaluate the 1D velocity models in their performance to simulate the observed records of the 21 Dec 1990 Mw 6.1 earthquake, at low frequencies (< 2 Hz). The best model was the one of Drakatos et al (2005), applicable to NW Greece, and we adopted it for our further calculations. We added a shallow layer of 1km in thickness, where the shear wave, Vs, velocity is 1200 m/s, representative of the NW (E1 in Figure 5) and central (E3 in Figure 5) part of the city, and Vs=2000 m/s for the southern part (E4 in Figure 5). These values have been determined previously (THALES-Project, 2015) to represent the engineering bedrock in the NW and central part of the city.

Figure 4 shows the hybrid motions for the scenario we examined. The results from COMPSYN and EXSIM were combined using the methodology proposed by Mai & Beroza (2003) in which a grid search is performed to identify the frequency where the two independently computed spectra exhibit the highest coherency, in terms of both the amplitude and the phase.

Table 1. Parameters and their values used in the simulations

Parameter	Value
Orientation of the fault (strike, dip)	strike 45°, dip 52° (rake -105°) [GCMT]
Dimensions of the fault (L, w)	Length 12 km; width 10 km
Depth of the upper edge of the fault	3.0 km
Stress drop (stress)	56 bars
Number of points for FFT (power of 2) leng1	4096
Sampling rate (dt)	0.005 sec
Shear wave velocity at the crust (beta)	3.4 Km/sec
Density of the crust (rho)	2.7 gr/cm ³
Attenuation model $Q(f)=Q_0 \cdot f^{\eta}$	$Q_0 = 88.0, \eta = 0.9$
Pulsing percentage	50 %

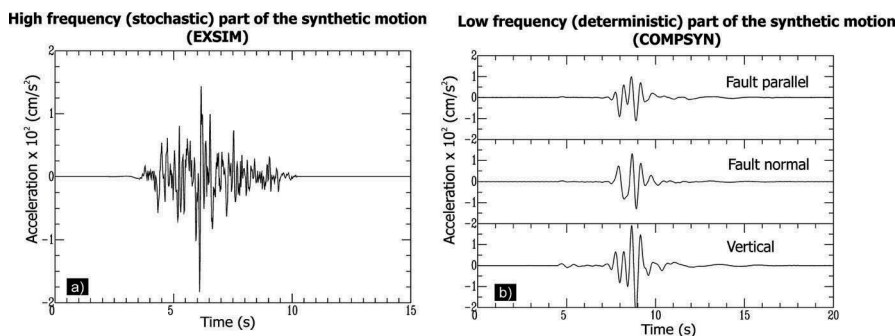


Figure 3. Synthetic ground motions for the scenario earthquake. a) Acceleration time series stochastically calculated using the code EXSIM. b) Acceleration time series ($f < 2$ Hz), obtained with a semi-analytical approach, using the code COMPSYN, that capture the near-field terms, calculated for rock outcropping.

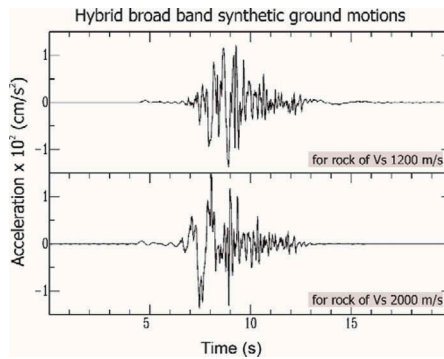


Figure 4. Hybrid broad band synthetic ground motions for the scenario earthquake obtained from spectral matching the stochastic HF component and the deterministic LF fault-normal component.

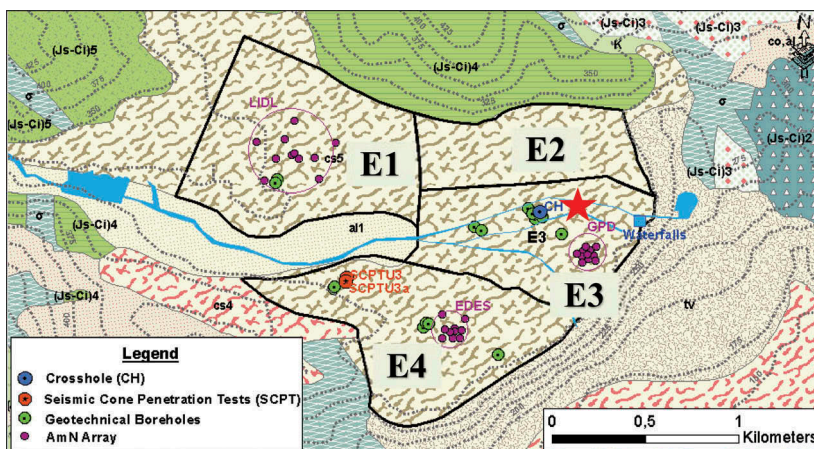


Figure 5. Geological map of Edessa (IGME Geological Map, scale 1:50.000) along with the topographic relief (grey dotted lines) and spatial distribution of geotechnical boreholes and geophysical measurements (Cross-hole: CH, Seismic Cone Penetration Tests: SCPTu, and Microtremor array measurements: LIDL, EDES, GPD). Black thick lines are used to show the different sectors of the urban area (E1-E4) adopted in the soil response analysis. The location of the Prefecture Building is at CH (red asterisk).

The synthesis of the two spectra was sought around 2 Hz (+/- 1Hz) and the largest coherency was identified at 2.7 Hz.

4 SITE SPECIFIC RESPONSE ANALYSIS

Besides source and path effects (discussed in the previous sections), seismic motion is also governed by the effect of local soil conditions at a site. To account for this effect, we used representative soil profiles (THALES-Project, 2015; Savvaidis et al., 2018) to perform 1D site response analyses. As input motions to the seismic bedrock, we used the recorded motions of the 1990 earthquake, deconvolved to the bedrock, and the hybrid motions, from the scenario earthquake.

4.1 1D soil profiles

Representative soil profiles for the city of Edessa were built on the basis of the available geological, geophysical and geotechnical data. An overview of these data can be found in Figure 5. Briefly, the urban zone of the city of Edessa is settled on Quaternary (Holocene) deposits

composed of contemporary and recent cones of torrential deposits, overlying Travertine that extends mainly at the northeastern, central and southern part of the study area. The geological bedrock in the area consists of Flysch at the northern and central parts and Limestone at the southern part of the considered area. Based on the available geotechnical information, quaternary deposits are mainly composed of silty sands and sandy silts at the northern part, and low plasticity clays, loose sandy silts and silty sands with gravels and/or organics and locally turf at the central part. At the southern part of the city, sediments have almost the same composition with those at the central part however with denser stratification, lower percentage of gravels and absence of organics and turfs. The correlation of geological and geotechnical data with geophysical measurements leads to the conclusion that sediments are stiffer in the northern part of the city (V_S : 450-550m/s) while their lowest V_S values are met in the central part (V_S : 150-500m/s). The presence of travertine formation is associated with V_S values of 950m/s and 650m/s, respectively at GPD and EDES sites, at depths greater than 15m and 20m and with an average thickness of 32m. Its spatial extent and thickness were empirically estimated based on the evaluation of its depositional process with respect to the alterations over the years of the Edessa riverbed. Finally, flysch at the north is revealed with V_S of 1100m/s, while limestone is interpreted with V_S values exceeding 2000m/s. The synthesis of these data determined the subdivision of the urban area to smaller ones (e.g. zones E1 to E4). For each one of zones E1, E3, and E4 and depending on the amount of available data, representative 1D soil profiles suitable for site response analysis were formed in such a way that: (a) the depth and thickness of the travertine formation was assigned to cover a variety of conditions, and (b) the uppermost layers stratigraphy and properties were fit to geotechnical and geophysical data available within each zone taking into account the dominance of the main geotechnical units with depth and average properties for each geotechnical unit that were indicated from the available boreholes.

Table 2 summarizes the representative 1D soil profiles at the central part (E3) of the city of Edessa. More details on the synthesis procedure as well as soil profiles for E1 & E4 zones can be

Table 2. Representative 1D soil profiles at the central part of the city of Edessa (zone E3).

No	Z ₁ (m) from	Z ₂ (m) to	U.S.C.S. /GEOLOGICAL UNIT	PI	N ₃₀ (SPT)	γ (kN/m ³)	Vs(m/s)
1	0.0	4.5	CL (SM)	13.2	8	19.0	150-250
	4.5	8.0	ML-OL		9	19.0	250
	8.0	10.5	SM		16	20.0	400
	10.5	12.5	ML		19	20.0	400
	12.5	13.5	CL-SM		14.5	20.0	400
	13.5	15.5	ML			30	20.0
	15.5	23.0	SM		27	20.0	500
	23.0	30.0	ML		20.0	550	
	30.0	45.0-60.0*	Tv		21.0	700	
	45.0-60.0	Infinite	Fa		22.0	1200	
2	0.0	4.0	CL	16.3	6	19.0	150
	4.0	7.0	SM-ML	16.5	5	19.0	250
	7.0	12.5	OL-Pt	NP	8	19.0	250-400
	12.5	15.0	ML-MH	NP	40	20.0	400
	15.0	25.0-40.0*	Tv	21.0	700		
	25.0-40.0	Infinite	Fa	22.0	1200		
3	0.0	3.0	CL - SC	12	13	20.0	200
	3.0	6.0	SM	NP	15	20.0	250
	6.0	9.0	Pt-OL	20.0	250		
	9.0	16.0	SM	NP	24	20.0	400
	16.0	20.0	SM	NP	37	20.0	500
	20.0	45.0-75.0*	Tv	21.0	700		
	45.0-75.0	Infinite	Fa	22.0	1200		

* Parametric estimation of the thickness of the Tv formation

found in Savvaidis et al. (2018). For the sake of comparisons with EC8 design spectra, presented in the following section, representative 1D soil profiles at all zones were categorized in EC8 soil types according to the parameter $V_{S,30}$. Despite the observed differences in soil material stratification at the top 30m of depth, all 1D soil profiles are categorized as EC8 soil type B.

4.2 Site response analyses – Methodology and results

Site response analyses of representative 1D soil profiles of E1, E3 & E4 zones were performed using the computer program STRATA (Kottke et al., 2008) that performs equivalent linear, EQL site response analysis (namely linear wave propagation with strain dependent dynamic soil properties) in the frequency domain using time domain input motions or random vibration theory (RVT) methods, and allows for randomization of the site properties.

Herein, time domain input motions were used and specifically the hybrid motions from the scenario earthquake presented in the previous paragraphs as well as the recorded motion of the 1990 earthquake (at CH site, i.e. the Prefecture Building, denoted in Figure 5), deconvolved, however, to bedrock conditions.

EQL site response analyses requires the use of appropriate shear modulus reduction and material damping curves for each layer that need to be selected in absence of site specific data. For this reason, sand, silt and clay layers were modeled using the $G-\gamma-D$ curves of Darendeli (2001) for soil types with similar physical and mechanical properties, while sandy and sandy gravel soil formations were modeled using the $G-\gamma-D$ curves proposed by Rollins et al. (1998) and corrected by Lavda (2009). With reference to organic soil layers, it is assumed that these layers are of low to medium organic content ($OC=30\%$) and the corresponding material curves of Kishida et al (2009) are used in the analysis.

Figure 6 summarizes the elastic site response acceleration spectra (for 5% critical damping computed) computed on the basis of the 1D soil profiles at (a) E1, (b) E3 and (c) E4 zones and their comparison with the elastic design spectra of EC8 for soil type B. In addition to the above, Figure 7 shows for all zones cumulatively (a) absolute and (b) normalized acceleration spectra with respect to computed peak ground acceleration (PGA) as well as (c) bi-normalized acceleration spectra with respect to both PGA and dominant period of ground motion (Tp).

The results indicate that site response characteristics of the examined soil profiles vary significantly despite the fact that all of them fall within EC8 soil category B. Observed variability is attributed to a) the intensity of the input motion and the corresponding degree of induced

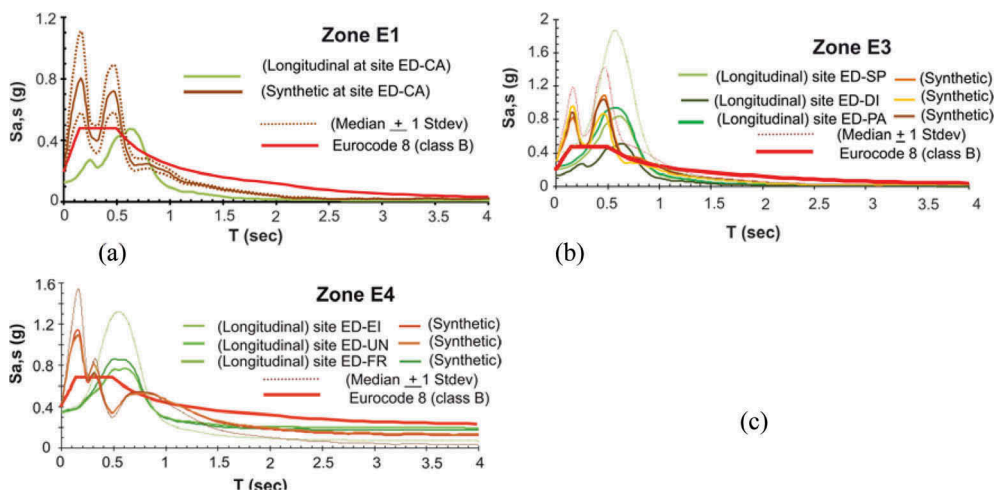


Figure 6. Elastic site response acceleration spectra (for 5% critical damping computed) computed on the basis of the 1D soil profiles at (a) E1, (b) E3 and (c) E4 zones and their comparison with the elastic design spectra of EC8 for soil type B.

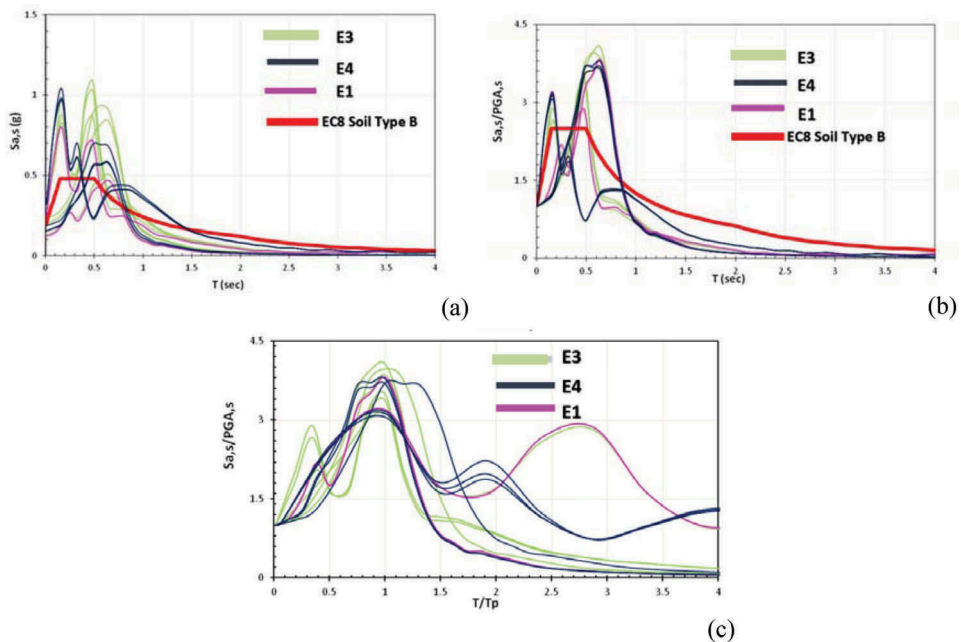


Figure 7. Site response analyses results: (a) absolute and (b) normalized acceleration spectra with respect to computed peak ground acceleration (PGA) as well as (c) bi-normalized acceleration spectra with respect to both the PGA and the dominant period of ground motion (T_P).

non-linearity in soil materials, as well as, b) its predominant period. The latter is clearly depicted in Figure 7c in which maximum values of bi-normalized acceleration spectra appear at the predominant period of input motion. Compared to EC8 soil class B elastic design response spectra, the results show that Edessa is susceptible to significant ground motion amplification during a seismic event which considerably exceeds design specification for the frequency band between 0.5 sec and 0.9 sec approximately.

5 CONCLUSIONS

Recognizing the fact that regions in northern Greece, which presently exhibit moderate to low seismicity, might not reflect the seismic potential of these areas, taking into account the uncertainties in the return periods of known faults, alongside the fact that many faults are not known, we studied the case of the city of Edessa, which belongs to the zone of lowest seismic hazard (design acceleration 0.16g) according to the national building code. We produced synthetic acceleration time histories for a pragmatic earthquake scenario, similar to that assumed in the national building code (Return Period, $T_r=475$ years). The scenario earthquake, of Mw6.05 on the South Almopia Fault and at a distance of 11 km from the center of Edessa, was selected based on a recent PSHA study and deaggregation of pertinent results for the area of interest (Thales-Project, 2015). Synthetics were produced using both a finite-fault stochastic simulation method (e.g. Motazedian and Atkinson, 2005; EXSIM code) and a deterministic approach (Spudich & Xu, 2003; COMPSYN code). The results of the two methods were finally combined toward hybrid synthetic acceleration time histories. Subsequently, the latter were used as input, along with the records of a past earthquake that caused damage to the town of Edessa (i.e. the 1990, Mw6.1 Goumenisa earthquake) in a soil response analysis. Representative soil profiles were suggested for the different parts of the urban area of Edessa and modified the common input motion differently. We concluded that site response

characteristics vary significantly across the urban area and that Edessa is susceptible to considerable ground motion amplification, which may lead to exceedance of design specification, especially within the period band 0.5-0.9 s. The above considerations indicate that site specific analyses on the basis of soil properties variability and realistic input motion for near fault scenario earthquakes are essential in the correct evaluation of the site response.

ACKNOWLEDGEMENTS

A. K and Z. R acknowledge partial support by the project “HELPOS – Hellenic System for Lithosphere Monitoring” (MIS 5002697), funded by “Competitiveness, Entrepreneurship and Innovation” (NSRF 2014-2020) and co-financed by Greece and EU (ERDF). Thanks are also due to all our colleagues, who contributed to the THALES “SITE-CLASSIFICATION” project.

REFERENCES

- Anderson, J. G. & Hough, S. 1984. A model for the shape of the Fourier amplitude spectrum of acceleration at high frequencies. *Bull. Seism. Soc. Am.* 74: 1969-1993.
- Caputo, R., Chatzipetros, A., Pavlides, S. & Sboras, S. 2012. The Greek Database of Seismogenic Sources (GreDaSS): state-of-the-art for northern Greece. *Annals of Geophysics* 55(5): 859–894.
- Darendeli, M. 2001. Development of a new family of normalised modulus reduction and damping curves. PhD thesis, *Rep. No. GD01-1*, University of Texas at Austin, Texas.
- Drakatos, G., Voulgaris, N., Pirli, M., Melis, N. & Karakostas, B. 2005. 3-D crustal velocity structure in Northwestern Greece, *PAGEOPH* 162: 37-51.
- Eurocode 8-ENV 1998-1-1: Design provisions for earthquake resistance of structures - Part 1-1: General rules - Seismic action and general requirements for structures.
- Kishida, T., Boulanger, R.W., Abrahamson, N.A., Wehling, T.M. & Driller, M.W. 2009. Regression models for dynamic properties of highly organic soils. *Journal of Geotechnical and Geoenvironmental Engineering* 135(4): 533-543.
- Klimis, N., Margaris, B., Anastasiadis, A., Koliopoulos, P. & Kirtas, E. 2006. Smoothed Hellenic Rock Site Amplification Factors, *5th Hellenic Congress of Geotechnical and Geoenvironmental Engineering, Vol. 2*, 239-246, *Xanthi, Greece* [in Greek].
- Kottke, R., & Rathje, E. 2008. Technical manual for Strata, *Report No.: 2008/10*. Berkeley: Pacific Earthquake Engineering Research Center, University of California.
- Lavda, A. 2009. Dynamic behaviour of gravelly soils, *MSc thesis, Imperial College London*, pp. 122.
- Mai, M. P. & Beroza, G. 2003. A hybrid method for calculating near-source, broadband seismograms: application to strong motion prediction, *PEPI* 137: 183-199.
- Margaris, B. & Boore, D. 1998. Determination of $\Delta\sigma$ and κ_0 from response spectra of large earthquakes in Greece, *Bull. Seism. Soc. Am.* 88: 170-182.
- Motazedian, D. & Atkinson, G. 2005. Stochastic Finite-Fault Modeling Based on a Dynamic Corner Frequency, *Bull. Seism. Soc. Am.* 95: 995-1010.
- Panagiotopoulos, D., Papadimitriou, E., Papaioannou, C., Scordilis, E. & Papazachos, B. 1993. Source properties of the 21 Dec 1990 Goumenisa Earthquake in Northern Greece, *Proc. 2nd Congress of the Hellenic Geophysical Union, 5-8 May 1993, Florina, Greece*.
- Papazachos, B. & Papazachou, K. 2003. *The earthquakes of Greece*, Thessaloniki: Ziti Publications.
- Pavlides, S. 1998. Dating the neotectonisms in south Almopias (central Macedonia, N. Greece), *Bull. Geol. Soc. Greece* 32 (1): 189-197.
- Savvaïdis, A., Makra, K., Klimis, N., Zargli, E., Kiratzi, A & Theodulidis, N. 2018. Comparison of Vs30 using measured, assigned and proxy values in three cities of northern Greece, *Engineering Geology* 239: 63-78.
- Spudich, P. & Xu, L. 2003. Software for calculating earthquake ground motions from finite faults in vertically varying media, *IASPEI handbook of earthquake and engineering seismology*, Amsterdam: Academic Press.
- THALES-Project Report, 2015. Characterization of site conditions in Greece for realistic seismic ground motion simulations: pilot application in urban areas, THALES MIS377355, (D8), Final Report.